Optical vortex trap for resonant confinement of metal nanoparticles

Maria Dienerowitz[*], Michael Mazilu, Peter J. Reece, Thomas F. Krauss and Kishan Dholakia

SUPA, School of Physics and Astronomy, University of St Andrews, St Andrews, Fife, KY169SS, United Kingdom
[*]Corresponding author: md60@st-andrews.ac.uk

Abstract: The confinement and controlled movement of metal nanoparticles and nanorods is an emergent area within optical micromanipulation. In this letter we experimentally realise a novel trapping geometry near the plasmon resonance using an annular light field possessing a helical phasefront that confines the nanoparticle to the vortex core (dark) region. We interpret our data with a theoretical framework based upon the Maxwell stress tensor formulation to elucidate the total forces upon nanometric particles near the particle plasmon resonance. Rotation of the particle due to orbital angular momentum transfer is observed. This geometry may have several advantages for advanced manipulation of metal nanoparticles.

©2008 Optical Society of America

OCIS codes: (140.7010) Laser trapping, (140.3300) Laser beam shaping, (240.6680) Surface plasmons, (350.4855) Optical tweezers or optical manipulation

References and links

1. S. Kühn, U. Hakanson, L. Rogobete, and V. Sandoghdar, "Enhancement of single-molecule fluorescence using a gold nanoparticle as an optical nanoantenna," Phys. Rev. Lett. **97**, 017402 (2006).
2. A. Csaki, F. Garwe, A. Steinbrück, G. Maubach, G. Festag, A. Weise, I. Riemann, K. König, W. Fritzsche, "A parallel approach for subwavelength molecular surgery using gene-specific positioned metal nanoparticles as laser light antennas," Nano Lett. **7**, 247-253 (2007).
3. F. Svedberg, Z. Li, H. Xu, M. Käll, "Creating hot nanoparticle pairs for surface-enhanced Raman spectroscopy through optical manipulation," Nano Lett. **6**, 2639-2641 (2006).
4. A. Ashkin, "Applications of laser radiation pressure," Science **210**, 1081-1088 (1980).
5. K. Svoboda and S. M. Block, "Optical trapping of metallic Rayleigh particles," Opt. Lett. **19**, 930-932 (1994).
6. P. M. Hansen, V. K. Bhatia, N. Harrit, and L. Oddershede, "Expanding the optical trapping range of gold Nanoparticles," Nano Lett. **5**, 1937-1942 (2005).
7. J. Prikulis, F. Svedberg, and M. Käll, "Optical spectroscopy of single trapped metal nanoparticles in solution," Nano Lett. **4**, 115-118 (2004).
8. M. Pelton, M. Liu, H. Y. Kim, G. Smith, P. Guyot-Sionnest, N. F. Scherer, "Optical trapping and alignment of single gold nanorods using plasmon resonances," Opt. Lett. **31**, 2075-2077 (2006).
9. K. C. Toussaint, M. Liu, M. Pelton, J. Pesic, M. J. Guffey, P. Guyot-Sionnest, and N. F. Scherer, "Plasmon resonance-based optical trapping of single and multiple Au nanoparticles," Opt. Express **15**, 12017-12029 (2007).
10. Y. Seol, A. E. Carpenter, and T. T. Perkins, "Gold nanoparticles: enhanced optical trapping and sensitivity coupled with significant heating," Opt. Lett. **31**, 2429-2431 (2006).
11. M. A. Clifford, J. Arlt, J. Courtial, and K. Dholakia, "High-order Laguerre–Gaussian laser modes for studies of cold atoms," Opt. Commun. **156**, 300-306 (1998).
12. L. Allen, M. W. Beijersbergen, R. J. C. Spreeuw, and J. P. Woerdman, "Orbital angular momentum of light and the transformation of Laguerre-Gaussian laser modes," Phys. Rev. A **45**, 8185-8189 (1992).
13. A. T. O'Neil and M. J. Padgett, "Three-dimensional optical confinement of micron-sized metal particles and the decoupling of the spin and orbital angular momentum within an optical spanner," Opt. Commun. **185**, 139-143 (2000).
14. J. W. Goodman, *Statistical Optics*, (Wiley-Interscience, 1985), p. 224.
15. D. McGloin, G. C. Spalding, H. Melville, W. Sibbett, and K. Dholakia, "Three-dimensional arrays of optical bottle beams," Opt. Commun. **225**, 215-222 (2003).
16. D. S. Bradshaw and D. L. Andrews, "Interactions between spherical nanoparticles optically trapped in Laguerre–Gaussian modes," Opt. Lett. **30**, 3039-3041 (2005).

17. M. Mansuripur, "Radiation pressure and the linear momentum of the electromagnetic field," Opt. Express **12**, 5375-5401 (2004).
18. J. P. Barton, D. R. Alexander, and S. A. Schaub, "Theoretical determination of net radiation force and torque for a spherical particle illuminated by a focussed laser beam," J. Appl. Phys **66**, 4594-4602 (1989).
19. A. Rohrbach and E. H. K. Stelzer, "Optical trapping of dielectric particles in arbitrary fields," J. Opt. Soc. Am. A **18**, 839-853 (2001).
20. J. P. Gordon, "Radiation forces and momenta in dielectric media," Phys. Rev. A **8**, 14-21 (1973).
21. L. Novotny and B. Hecht, *Principles of Nano-Optics*, (Cambridge University Press, 2006) p 404-428.
22. G. Mie, "Beiträge zur Optik trüber Medien, speziell kolloidaler Metallösungen," Ann. d. Physik **4**, 378-445 (1908).
23. P. B. Johnson and R. W. Christy, "Optical constants of the noble metals," Phys. Rev. B. **6**, 4370-4379 (1972).
24. M. Nieto-Vesperinas, P. C. Chaumet, and A. Rahmani, "Near-field photonic forces," Phil. Trans. R. Soc. Lond. A **362**, 719-737 (2004).
25. C. S. Adams and E. Riis, "Laser cooling and trapping of neutral atoms," Prog. Quantum Electron **21**, 1-79 (1997.)
26. I. Brevik, "Experiments in phenomenological electrodynamics and the electromagnetic energy-momentum tensor," Phys. Rep. **52**, 133-201 (1979).

1. Introduction

Nanometre-sized metal particles are a remarkable tool for various applications. They may enhance fluorescence and offer an extremely precise instrument for molecular surgery on chromosomes [1, 2]. In addition, trapping colloidal silver nanoparticles opens up new possibilities for Surface-Enhanced Raman Spectroscopy (SERS) [3]. In the domain of optical micromanipulation, it is a common misconception that optical tweezing of metal nanoparticles cannot readily be achieved [4]. In 1994 Svoboda and Block performed a key study showing optical trapping of metallic Rayleigh particles [5]. Subsequent investigations consider the size range of gold nanoparticles that can be stably trapped and manipulated in three dimensions, demonstrating trapping down to 18nm in size [6]. This offers an immense potential to explore fundamental physics of the resonant properties of metal nanoparticles: for example the effects of the interaction between two or more nanoparticles or the wavelength dependent resonance of nanorods [7-9].

The manipulation of metal nanoparticles may be considered in the intermediate regime between atom trapping and tweezing of micron-sized dielectric beads. Compared to large dielectric beads, optical tweezing of very small particles poses a significant challenge as the force necessary to trap, namely the gradient force F_{grad}, decreases with particle volume (and polarisability α). However, metal nanoparticles have an increased polarisability α when compared to their equivalently sized dielectric counterparts. In turn, this means we can tweeze metal nanoparticles more readily than nanometric sized dielectric particles. The concept of a plasmon resonance is distinct to nanoparticles with free electrons and thus not present in dielectric beads. Indeed, plasmon based trapping is an emergent area [8,9] but has not been applied to spherical nanoparticles nor exploited for trap geometries other than conventional single beam gradient tweezers.

In this letter, we investigate the interplay of the forces acting upon gold nanoparticles when exposed to laser light close to their plasmonic resonance. In particular we exploit the plasmon resonance for the first time to trap a nanoparticle within the dark core of a Laguerre-Gaussian (LG) light field using the scattering force to our advantage. This opens up new avenues for optical manipulation of metal nanoparticles beyond the single beam tweezers and presents a possibility to avoid potential heating [10] by trapping the nanoparticles away from the high intensity region of the trapping laser. The experimental realisation of the trap is firstly discussed before we progress to theoretical considerations and calculations for such a trapping geometry.

We demonstrate experimentally an optical trap exploiting the resonant properties of gold nanoparticles to explore the interaction with light around resonance. A theoretical analysis of our experimental geometry is discussed in the last section of our paper. Such a trap requires optical beamshaping in a manner such that we may confine the nanoparticle to a dark region enclosed by light. To achieve this, we use an annular light field that encapsulates the gold

nanoparticle, restricting its motion to the dark core. Single ringed (radial index *p=0*) Laguerre-Gaussian (LG) laser beams offer the advantage of such annular fields, whose size depends upon the azimuthal index ℓ (where ℓ is an integer number) [11]. The azimuthal phase index ℓ gives the number of 2π cycles in azimuthal direction around the circumference of the beam and is sometimes called the helicity or charge of the beam [12]. The distinct phase structure of such an LG beam leads to a phase singularity on the beam axis (vortex) with zero light intensity for beams with $\ell > 0$. Due to its helical wavefronts, the Poynting vector has an azimuthal component resulting in an orbital angular momentum of $\ell\hbar$ per photon. By employing LG beams of different azimuthal indices, the area of the dark core can be controlled and the number of confined particles is experimentally adjustable. The advantage of confinement is that particles remain in the dark region hence avoiding strong absorption and heating.

We note that micron-sized metallic particles have been trapped using annular light profiles [13] but in such a case, stress that no resonance is involved: as metallic particles increase in size, up to several hundred nanometres, their optical response includes contributions of higher order terms and multiple overlapping resonances. Even larger particles, in the micron-size regime, are more appropriately considered as highly reflective geometrical objects: the physical rationale and interpretation for trapping nanometric sized particles which we consider here is wholly different from that for micron-sized particles [13].

2. Experiment

Experimentally the Laguerre-Gaussian beam is generated with a blazed phase hologram (24% efficiency) placed in the laser beam path. We used *s*-polarised light of 528nm, 514nm, 488nm (from an Argon Ion laser) for our trapping studies. The generated LG beam is directed into a custom-built inverted microscope setup focusing the beam into the sample chamber with a 50x Nikon microscope oil immersion objective (Plan, 50x, 0.9 NA). Koehler illumination [14] of the sample was employed to obtain bright-field images with maximum contrast, which was crucial for subsequent particle tracking. Two microscope cover slips form the thin (7-10 microns deep) sample chamber containing the gold nanoparticles. The particle motion is viewed in transmission and its image recorded with a CCD camera (Watec, WAT250D). We used monodispersed gold nanoparticles suspended in deionised water (British Biocell) with diameters of 100nm and 250nm for our experiments. However, the 250nm gold nanoparticle is comparable to the laser wavelength employed in our experiment. It exhibits higher order resonances and thus forms a more complex system requiring the theoretical approach of the full Maxwell stress-tensor method which we discuss in the next section. Therefore we have restricted the majority of our experiments to 100nm gold nanoparticles although we note that 250nm nanoparticles could also readily be confined in the dark region of our trap.

We experimentally examined the interaction of gold nanoparticles with trapping light at 488nm, 514nm and 528nm. The position of the plasmon resonance for 100nm gold nanoparticles in water is around 580nm. The applied laser wavelengths are thus blue-detuned with respect to the plasmon resonance of the gold nanoparticles. The gold nanoparticles are confined within a region of a radius from 0.9 μm to 1.4 μm in the x-y plane. Their upward (axial) motion is restricted by the top glass cover slip. Below the trapping position the LG beam is focussed so tightly that the particles can not fall through the focus and get repelled upwards in direction of the beam propagation. A possibility to extend this new trapping geometry into a three dimensional trap would be to use a bottle beam geometry [15]. We readily achieved trapping of the 100nm gold nanoparticles at all three applied wavelengths. We also observed that the particle residence time in the dark core increased as we moved to higher laser powers.

At 528nm trapping can already be achieved for only 40mW of laser power whereas for 488nm at least 60mW is required. Because 528nm is closer to the particle plasmon resonance of the nanoparticles, where the scattering cross section is larger and the interaction with light

stronger, we have to employ less laser intensity to obtain equal confinement and trapping times compared to 514nm and 488nm. The trapping times increased from about 10s to several minutes when raising the power level at each wavelength. The laser power was measured at the back aperture of the trapping objective. To load the trap we temporarily block the trapping beam or rapidly move the stage such that the Stokes forces overcome any optical forces present, causing the nanoparticle to be loaded in the trap site. Only on a very few occasions, did the 100nm nanoparticles enter the trap without external help. However, they were able to escape the trap in an easier manner than they are able to enter. This behaviour suggests that the nanoparticles are not deeply confined and have to overcome a potential well before they enter the trap. Our theoretical analysis in section 3 confirms this concept which is seen in Fig. 4. Besides, the 250nm particles are more stably trapped than 100nm particles, an observation which is also validated by our calculations in the next section. As the size of the dark core of the LG beam is wavelength dependent, e.g. smaller for shorter wavelengths, the trapping region of the gold nanoparticles could be adjusted without changing the azimuthal phase index ℓ of the beam.
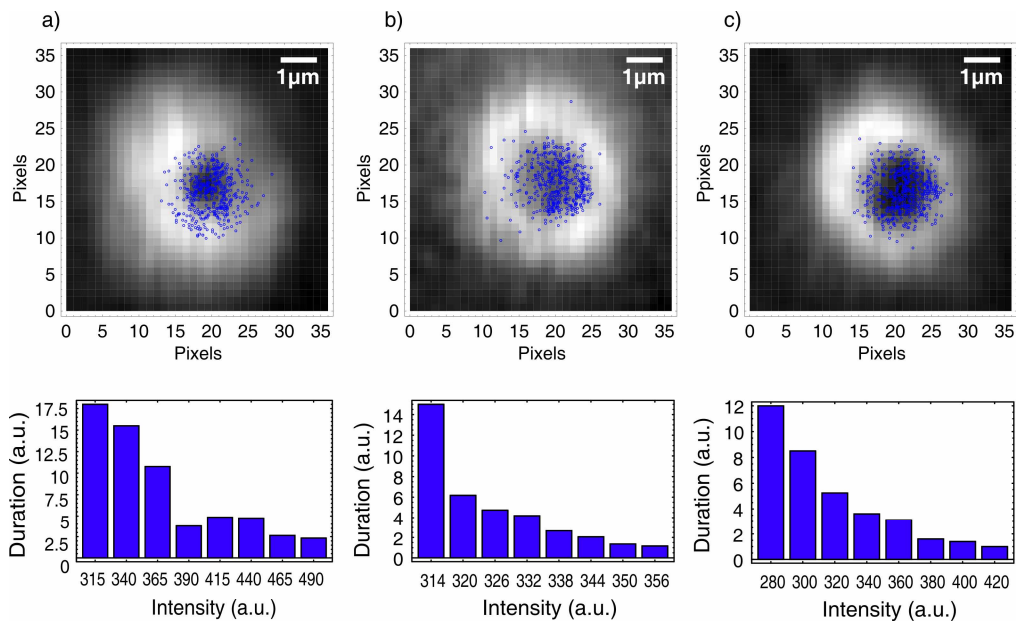

Fig. 1. (top) Spatial data points tracing the movement of a single gold nanoparticle confined to Laguerre-Gaussian beam with $\ell = 2$ and various wavelengths a) 488nm at 120mW, b) 514nm at 90mW and c) 528nm at 90mW laser power measured at the back aperture of the trapping objective. (bottom) The plots represent the average visit duration of a gold nanoparticle at a pixel site with certain intensity. Higher numbers correspond to a higher intensity. The histograms clearly show the nanoparticle's preference to reside within the regions of lowest intensity. The escape probability due to Brownian motion and radial acceleration because of the angular momentum is higher for lower laser powers. One pixel equals 200nm, thus the particles are confined to a region with a radius of 0.9 µm to 1.4 µm in our experiment.

We analysed the recorded video images of the particle motion with particle tracking software. The accuracy of this method is determined by the image quality which is limited by the size of the gold nanoparticles. Representative data extracts for each applied wavelength are shown in Fig. 1. In the first row we plot the positions of the gold nanoparticle with respect to the LG beam. Analysing the intensity level of each pixel visited by the nanoparticle and the relative duration of a visit yields the presented histograms in the second row. There is clear evidence of confinement within the low intensity regions of the LG beam.

In addition to the confinement of the particles, we observed the transfer of orbital angular momentum from the Laguerre-Gaussian beam to the particle. Once particles are caged by the Laguerre-Gaussian beam, they rotate around the beam propagation axis within the dark core of the beam. The sense of nanoparticle rotation remains the same and results from the transfer of orbital angular momentum (OAM) of the beam to the particle. We believe these are the smallest particles to date set into rotation by OAM transfer. The very fact such rotation around the beam propagation axis is observed is a strong indication that scattering between the light field and particle is the dominant interaction mechanism. Orbital angular momentum is a distinct feature of the LG beam and exists in parallel to spin momentum, analogous to spin and orbital momentum in atomic systems. The sense of the rotational motion of the gold nanoparticle within the trap was reversed when changing the sign of the azimuthal index ℓ. As expected, the rotation rate increases linearly with respect to laser power, with a maximum rate of 3.6Hz at 110mW for 514nm. We found a linear dependence of the rotation rate on power of about 33Hz/W. These results imply that the scattering force is the dominant interaction mechanism between the laser beam and gold nanoparticle, as orbital angular momentum is typically transferred by scattering.

The motion of two nanoparticles inside the trap was also interesting. The particles did not attract each other nor coagulate as usually seen in conventional optical tweezers; rather repulsion between the particles was consistently observed (Fig. 2). Two confined nanoparticles rotate together within the dark core of the Laguerre-Gaussian beam by keeping the largest distance possible, mostly 180° apart. We assign this behaviour to an optical binding type interaction which is the subject of further study [16].
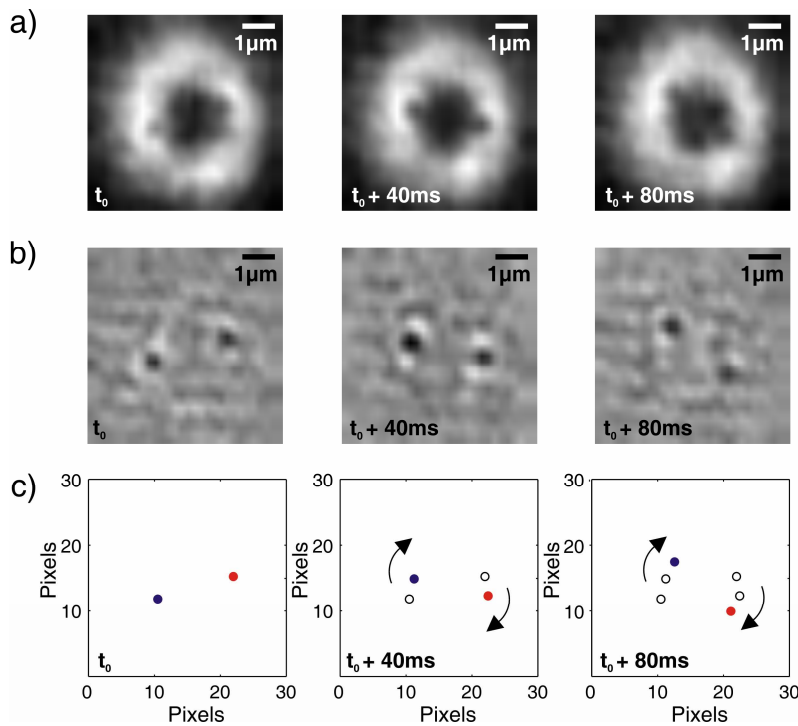

Fig. 2. Three subsequent pictures illustrating the rotation of two trapped 100nm gold nanoparticles due to orbital angular momentum (OAM) transfer. The particles are confined to the Laguerre-Gaussian beam but the strong "binding" repulsion between the spheres does not allow them to interact in the middle of the dark core. Together they rotate clockwise, retaining a separation angle of 180°. Displayed in row (a) are the noise-reduced movie stills out of a video sequence that are further processed with a background subtraction in row (b).

3. Theory

There are a number of ways to calculate the forces upon a particle within an optical trap including the Lorentz force formalism [17], the Maxwell stress tensor method [18] and the popular decomposition into scattering and gradient forces [19]. The latter is widely used [5,6,9] and, in general, combined with Mie theory. However, the gradient force is based on a dipolar model [20] and provides accurate results in the Rayleigh regime with $a \leq \lambda / 20$ where a is the particle diameter. The decomposition into scattering and gradient forces can thus only serve as a qualitative description of our experiment as $a \approx \lambda / 5$. Nonetheless, this approach gives an intuitive picture of the physical insight which is in particular valuable to understand the complex processes close to resonance. Following the qualitative discussion we calculate the total force acting on the gold nanoparticle by applying the Maxwell stress tensor model. This method is a very general approach remaining valid regardless of the particle shape and index of refraction and is not limited to the Rayleigh regime. In particular, it can be applied to absorbing and resonant metal nanoparticles and to the best of our knowledge has never been implemented for such a study.

3.1 Scattering and gradient force decomposition

We may assign components of the total force to the gradient force F_{grad}, the scattering force F_{scat} and the absorption force F_{abs}

$$
\begin{aligned}
F_{grad} &= \frac{1}{2} \ \alpha'(\omega) \ \nabla \langle E^2 \rangle \ , \\
F_{scat} &= n/c \ \langle S \rangle \ C_{scat} \ , \\
F_{abs} &= n/c \ \langle S \rangle \ C_{abs} \ ,
\end{aligned}
\tag{1}
$$

where $\alpha(\omega) = \alpha'(\omega) + i\alpha''(\omega)$ is the particle's complex polarisability [6,21]. S refers to the Poynting vector, n the refractive index of the host medium and c the speed of light. C_{scat} denotes the scattering cross section of the nanoparticle and C_{abs} its absorption cross section. Both are strongly wavelength dependent for metal nanoparticles and may be calculated with Mie theory [22]. The cross sections can be expressed in terms of the polarisability as

$$
\begin{aligned}
C_{scat} &= \frac{k^4}{6\pi\varepsilon_0^2} \ |\alpha(\omega)|^2, \\
C_{abs} &= \frac{k}{\varepsilon_0} \ \alpha''(\omega) \ ,
\end{aligned}
\tag{2}
$$

where k denotes the wave vector in the host medium [21]. The polarisability α, as well as the scattering and absorption cross sections, gives a first qualitative description for the forces acting on the nanoparticle. F_{grad} is linearly dependent on the real component of the polarisability α'; F_{scat}, and F_{abs} depend linearly upon the scattering and absorption cross sections. The plasmon resonance of the metal nanoparticle emerges in the polarisability α and cross sections C_{scat}, C_{abs} (Fig. 3). The position of the resonance with respect to wavelength results from size, shape, and material properties and is situated in the visible for gold nanoparticles. Excitingly, a metal nanoparticle at resonance gives rise to large field enhancements in the proximity of the nanoparticle and strong interaction processes with other particles. The plasmonic resonance is the mutual basis of all the important and emergent applications for metal nanoparticles.

  Although the plasmonic resonance is not as sharp and distinct as an atomic resonance on a typical dipole transition, the nanoparticle's properties vary significantly when interacting with light near or far from such a resonance. Notably, there are subtle differences to the atomic regime, for example in the process of light scattering. In the atomic regime, scattering is

evidently connected to absorption and reemission of photons, and therefore associated with unwanted heating processes. With nanoparticles a distinction between purely absorptive (and therefore heating) and scattering processes is made.

A metal nanoparticle may either be attracted or repelled by a trapping laser [24]. Attraction is based upon the gradient force and is the key process for optical tweezing. Repulsion can occur as a result of two different effects: a repulsive gradient force which is attributed to a negative real part of the polarisability α' or a dominating scattering force. The repulsive gradient force is often exploited in atom trapping by using a so-called blue-detuned trap confining the atoms within a low intensity region of the trapping laser [25].
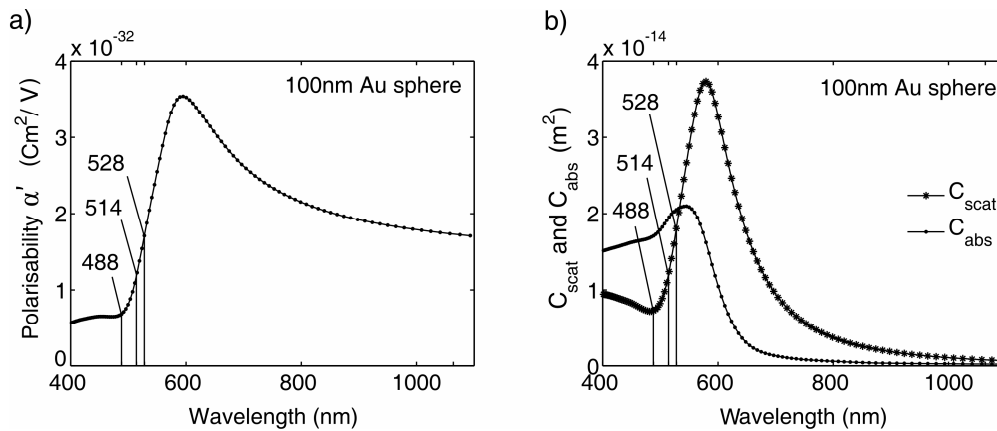
a)

b)

Fig. 3. (a). The real part of the polarisability α' of a 100nm gold sphere calculated with the scattering C_{scat} and absorption cross section C_{abs} from Mie theory (see equation 4) and permittivity values from Johnson et al. [23]. α' and thus F_{grad} is decreased by 30% and 70% for 488nm, 514nm and about the same at 528nm as compared to 1064nm. (b) C_{scat} and C_{abs} of a 100nm gold sphere calculated with Mie theory plotted against the wavelength of excitation. The increase of C_{scat} at the applied wavelengths of 488nm, 514nm and 528nm as compared to 1064nm is evident

It has been shown repeatedly that metal nanoparticles can be tweezed in the high intensity region of the trapping laser utilising a wavelength of 1064nm, far above resonance in the infra-red. However, it is impossible to tweeze a metal nanoparticle at a wavelength just below its resonance. This effect has already been mentioned elsewhere and is an indication that metal nanoparticles are repelled by the high intensity regions of the beam at particular wavelengths [7,8]. These observations suggest that the forces exerted on the metal nanoparticles are strongly wavelength dependent and it is vital to choose the correct wavelength in order to achieve optical tweezing.

The optical properties of gold differ from those of an ideal metal. Gold absorbs more than for example silver and its particle plasmon resonance is strongly damped. The real part of the polarisability $\alpha'(\omega)$ of a 100nm gold particle is therefore never negative and hence does not support the idea of a repulsive gradient force (Fig. 3). In short, one finds that for silver nanoparticles or gold nanorods the gradient (dipole) force may be repulsive, but for spherical gold particles it is always attractive. However, the real component of the polarisability is reduced below the resonance compared to its value above the resonance. More importantly the scattering cross section is substantially increased below the resonance: at 488nm about 10times, at 514nm about 16times and at 528nm about 23times as compared to 1064nm (Fig. 3). We conclude that the gradient force F_{grad} is not able to overcome the resonantly enhanced scattering force at the wavelengths applied. Therefore gold nanoparticles are repelled by the high intensity regions of the beam as the scattering dominates the interaction process. The basis of the gold nanoparticle trap in our experiment is thus primarily the resonantly

enhanced scattering force. This conclusion is in agreement with the total force calculations described in the following section.

3.2 Maxwell's stress tensor approach

We calculate the total optical force acting on the particle by integrating Maxwell's stress tensor on a surface surrounding the particle. In a host material the stress-tensor $\overline{\overline{T}}$ is given by [26]

$$\overline{\overline{T}} = \vec{D} \otimes \vec{E}^* + \vec{B} \otimes \vec{H}^* - \frac{1}{2}(\vec{D} \bullet \vec{E}^* + \vec{B} \bullet \vec{H}^*), \tag{3}$$

with $\vec{E}$, $\vec{D}$, $\vec{H}$ and $\vec{B}$ denoting the electric field, the electric displacement, the magnetic field and magnetic flux respectively. Applying the constitutive relations $\vec{D} = \varepsilon_r \varepsilon_0 \vec{E}$ and $\vec{B} = \mu_r \mu_0 \vec{H}$ with $\mu_r = 1$ and using SI units we find

$$T_{ij} = \varepsilon_r \varepsilon_0 E_i E_j^* + \mu_r \mu_0 H_i H_j^* - \frac{1}{2} \sum_k \left(\varepsilon_r \varepsilon_0 E_k E_k^* + \mu_r \mu_0 H_k H_k^* \right). \tag{4}$$

The optical force acting on the nanoparticle, averaged over one optical cycle, is

$$\vec{F} = \frac{1}{2} \mathrm{Re} \left(\int_S \overline{\overline{T}} \bullet \vec{n} \; ds \right), \tag{5}$$

where $\vec{n}$ is the normal vector pointing outward to the surface *S* surrounding the particle. Here we have averaged over one optical cycle.

We use a finite element method to calculate the different fields around the 100nm gold nanoparticle under LG beam illumination (as described in the experimental section). The radial optical force determines the transversal confinement of the particle inside the annular beam. It is this radial force that we use in Fig. 4 to calculate the integrated optical work needed for the particle to escape from the optical trap. The figure shows the trapping potential after the focal plane. Nanoparticles of 100nm and 250nm have to overcome a potential barrier to enter the trap. Once inside the trap they are confined within the dark region of the Laguerre-Gaussian beam. The black curve in Fig. 4 shows that, for 100nm nanoparticles, the trapping potential is shallow and therefore confirms the experimental observation that the trapping is less stable for 100nm particles compared to 250nm particles. The trapping potential for 250nm nanoparticles is deeper and hence results in a stronger trap as mentioned in the experimental section. Also, the area of confinement of about 2μm in diameter agrees with our experimental data. The grey region in Fig. 4 represents the intensity profile of the beam. We remark that, based on our theoretical model, small nanoparticles - 50nm and 70nm - are easier to trap.
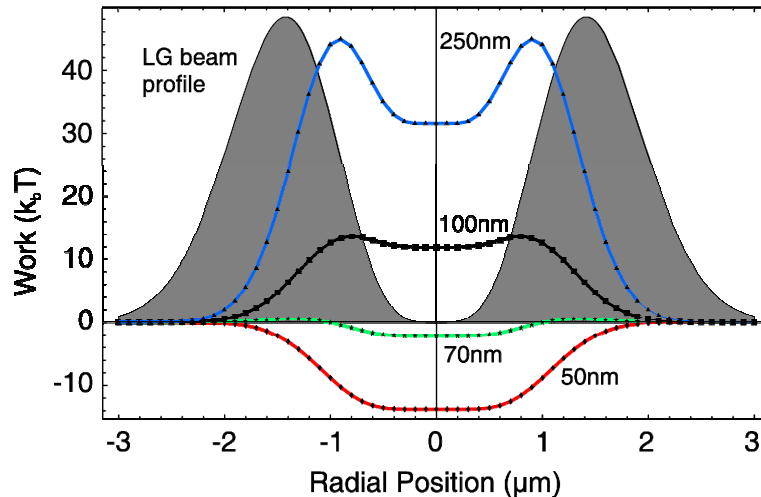
Fig. 4. The lines correspond to the optical trapping potential (work) in the radial direction for 50nm, 70nm, 100nm and 250nm gold particles in an LG beam (ℓ =2) 1µm after the focal plane. The grey shaded area denotes the LG beam intensity profile. The LG beam has a waist of w_0=1000nm, 100mW power and a wavelength of 528nm. The work is in units of k_bT where k_b is the Boltzmann constant and T the temperature of the bath (T=20⁰C).

4. Conclusion

In conclusion, we have demonstrated a new trapping geometry for gold nanoparticles that exploits their plasmonic response and confines them to a dark region of an annular Laguerre-Gaussian light field. Due to a significant increase of the scattering force on the blue-detuned side of the resonance, the total force acting upon the particle is repulsive. This offers new possibilities for manipulating metal nanoparticles whilst restricting them to a dark region away from the trapping laser, thus potentially avoiding strong heating. Orbital angular momentum was transferred from the LG beam to the nanoparticles. We theoretically analysed the optical forces acting on nanoparticles in the LG beam using a rigorous Maxwell stress-tensor method. Our theoretical considerations showed that blue-detuned trapping for gold nanoparticles is based upon a resonantly enhanced scattering mechanism. Future studies will explore silver nanoparticles where the repulsive force is predicted to be due to dipole interactions as well as more detailed investigations of the behaviour of multiple particles within the trap.

Acknowledgments